3

Nanostructured Systems for Biological Materials

Esther H. Lan, Bruce Dunn, and Jeffrey I. Zink

Summary

The sol-gel process is a chemical technique for immobilizing biomolecules in an inorganic, transparent matrix. The dopant biomolecules reside in an interconnected mesoporous network and become part of the nanostructured architecture of the entire material. In this chapter, we review the sol-gel immobilization approach and discuss how it leads to the stabilization of a number of proteins against aggressive chemical and thermal environments. We also review the sensor applications of this material that result from having analyte molecules diffuse through the matrix and reach the immobilized biomolecule.

Key Words: Sol-gel; aerogel; xerogel; sol-gel encapsulation; butyrylcholinesterase; creatine kinase; cortisol.

1. Introduction

There are a variety of methods for immobilizing biomolecules including entrapment, microencapsulation, covalent attachment, and adsorption. In this chapter, we review our work involving an immobilization process that has features common to both entrapment and microencapsulation. In this method, biomolecules are encapsulated in the pores of an inorganic material that is prepared using sol-gel chemistry, one of a variety of "soft chemistry" approaches in which solid-state materials are synthesized at room temperature under mild conditions. The resulting matrix constitutes a nanostructured material. It possesses two phases: there is a network of solid colloidal particles arranged with interpenetrating mesoporosity that is filled with the solvent phase. The dopant biomolecules reside in the mesoporous network, in a solvent-rich environment, and become part of the nanostructured architecture of the entire material.

The nanostructure of the material has a profound effect on properties. When the molecular sizes of the dopant molecules are less than the average pore

From: *Methods in Molecular Biology, vol. 300:*
Protein Nanotechnology, Protocols, Instrumentation, and Applications
Edited by: T. Vo-Dinh © Humana Press Inc., Totowa, NJ

diameter, these molecules (usually of low molecular weight) are mobile within the solvent-filled pores. The high molecular weight biomolecules, however, are confined within the cages formed by the developing sol-gel nanostructure. The biomolecules have local mobility, but no translational mobility. A diverse range of proteins has been immobilized in sol-gel-derived materials including globular and membrane-bound proteins, enzymes, and other biosystems. In almost all cases, the chemistry of the dopant biomolecule in the nanostructured environment is analogous to that in solution, with the subtle difference being that now the system involves a porous inorganic matrix. The properties of both the solid phase and the solution phase are evident in the sol-gel-encapsulated materials, and frequently it is the interactions of the dopant biomolecules with the sol-gel matrix that determine the reaction pathways for a particular biological system.

In this chapter, we first review the basic aspects of sol-gel chemistry and their application to the encapsulation of biomolecules. Then we review the details of protein stabilization, one of the most significant properties provided by sol-gel encapsulation. After reviewing the different types of stabilization, we detail the remarkable encapsulation properties of creatine kinase. Finally, we present recent research in our laboratory in which we have combined organic and biological molecules in sol-gel matrices to achieve greater functionality. The latter work is directed at sensor applications.

1.1. The Sol-Gel Process

The sol-gel process is a low-temperature synthesis technique for producing amorphous inorganic solids, i.e., glasses. A sol is generally defined as a colloidal solution with particles of <100 nm suspended in a liquid, whereas a gel is a semisolid colloid. One of the distinct advantages of the sol-gel process is that glasses can be prepared at room temperature with excellent homogeneity and high purity. The glasses fabricated using this process are highly porous, so that selected dopants can be incorporated into the porous glass matrix. Moreover, it is possible to make these sol-gel materials optically transparent, so that they can be used as sensors. There has long been considerable interest in making transparent glasses that contain various organic and inorganic dopants, and the ability to make glasses at low temperatures is extremely useful because many dopants undergo irreversible changes at high temperatures.

In the sol-gel process, a colloidal sol forms from the hydrolysis and polycondensation of metalorganic precursors. The precursors are typically metal alkoxides, $M(OR)_n$, in which OR is OCH_3 (methoxy), OC_2H_5 (ethoxy), and so on. The most commonly used alkoxides for making silica-based materials are tetramethoxysilane (TMOS) (OR = OCH_3) and tetraethoxysilane (OR = OC_2H_5), because hydrolysis and condensation can be well controlled. An over-

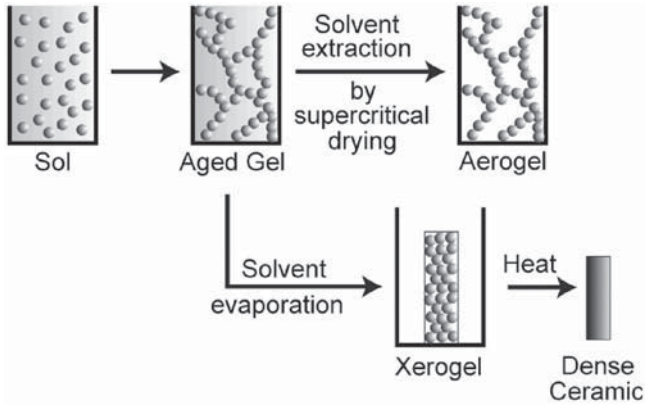

Fig. 1. Overview of sol-gel processing in fabrication of wet (aged) gels, aerogels, and xerogels. (Adapted from **ref. *4***.)

view of the sol-gel process can be divided into the following steps: sol formation, gelation, drying, and densification, as illustrated in **Fig. 1**. As can be seen, the method of drying (solvent evaporation or extraction) can greatly affect the final matrix structure, pore size, and pore volume. The resulting material can be in the form of a monolith, thin film, or fiber, depending on the fabrication method.

In the hydrolysis reaction, the precursor (metal alkoxide) is mixed with water in the presence of a catalyst. An alcohol can be added as a cosolvent since alkoxides and water are immiscible, but both are soluble in ethanol and methanol. The hydrolysis step leads to formation of silanol groups (Si-OH), which are intermediates, and alcohol as a byproduct. Hydrolysis is followed by condensation, as silanol groups condense to form siloxane groups (Si-O-Si), releasing alcohol or water as a byproduct. Note that the hydrolysis and condensation reactions occur concurrently. Both of these reactions are depicted in **Fig. 2**.

A variety of factors affect the hydrolysis and condensation reactions and final microstructure of the gel. These factors include the solution pH, temperature, nature of alkoxide, amount of alcohol, ratio of alkoxide to water to alcohol, and type of catalyst used. The relative rates of hydrolysis and condensation determine the final structure of the gel ***(1)***, and there have been extensive studies on the effect of these factors on the polymerization reactions and final microstructure ***(1–5)***. The final structure of the glass can be controlled to a large degree by controlling the hydrolysis and condensation reactions. A fast hydrolysis and slow condensation favor formation of more highly condensed silicate polymers, whereas slow hydrolysis and fast condensation result in less

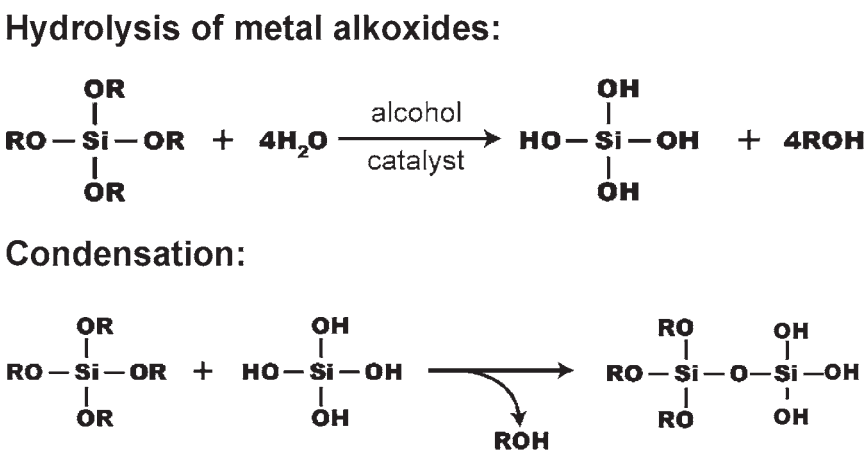

Fig. 2. Hydrolysis and condensation reactions in sol-gel processing.

condensed polymers *(2)*. The ratio of water to metal alkoxide, in which r_w = [water]/[metal alkoxide], can also be used to tailor the gel network. For $r_w < 4$, the structure is primarily that of linear polymers, whereas if $r_w > 4$, the structure is primarily crosslinked, three-dimensional (3D) networks *(5)*. Another critical factor controlling gel structure is pH. Silicate sols prepared under acidic conditions (acid catalyzed) form primarily linear polymers, and on drying, a dense gel forms with relatively small pores (**Fig. 3A**). On the other hand, silicate sols prepared under basic conditions (base catalyzed) form primarily branched clusters, and on drying, the gel network is more open, with a larger pore network (**Fig. 3B**) *(3)*.

As hydrolysis and condensation polymerization reactions continue, the sol becomes a gel. The gelation point is defined as the time at which the silica matrix forms a continuous solid *(6)* or the point at which the material can support a stress elastically *(1)*. After the sol-to-gel transition, there is a sharp increase in viscosity and the polymer structure becomes rigid. The sol-to-gel transition is irreversible, with essentially no change in volume. The material after gelation is composed of two distinct phases: amorphous silica particles (5–10 nm in diameter) and an interstitial liquid phase *(6)*. This material is described as a "wet" gel, as long as the interstitial liquid phase (i.e., pore liquid) is maintained. As the gel ages, polycondensation continues, increasing the connectivity of the network, and its structure and properties continue to change.

It is possible to prepare sol-gel materials in a wide range of geometries, from bulk monolith materials (dimensions >1 mm) to thin films (thickness of

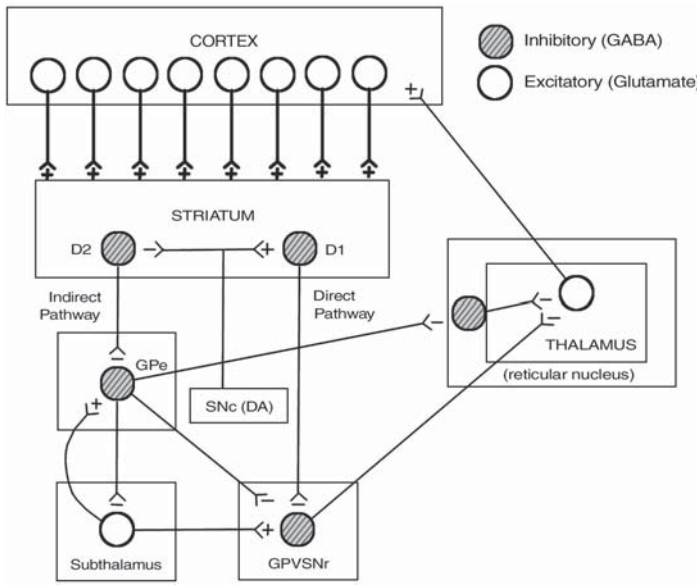

Fig. 3. **(A)** Acid catalysis in sol-gel processing of silica leads to primarily linear polymers, and upon drying, a dense gel forms with relatively small pores. **(B)** Base catalysis in sol-gel processing of silica leads to primarily branched clusters, and on drying, the gel network is more open, with a larger pore network. (Adapted from **ref. *3***.)

tens to hundreds of nanometers). In the fabrication of these materials, if the pore liquid is allowed to evaporate, the gel begins to dry. The drying process is accompanied by considerable weight loss and volume shrinkage. Typically, gel drying is accomplished under ambient conditions. As the interstitial liquid evaporates from the pores, there are large capillary forces, causing pore collapse and material shrinkage. The dried gel is described as a "xerogel" (*see* **Fig. 1**). For silica sol-gel materials, xerogels are typically ≤50% of their original volume. Alternatively, solvent extraction can be performed using supercritical drying. This supercritically dried gel is called an "aerogel" (*see* **Fig. 1**). Under these conditions, pore liquid can be removed without pore collapse and subsequent shrinkage, resulting in a lightweight material with relatively large pore sizes and high pore volume.

2. Encapsulation of Biomolecules in Sol-Gel Matrices

The encapsulation of proteins and other biomolecules in sol-gel-derived glasses is an intriguing research area because it involves placing delicate biological molecules with well-defined structures in the pores of a matrix that is, by comparison, hard and disordered. The encapsulation of biomolecules in sol-

gel-derived glasses has been ongoing for more than a decade, with the first research in this area published in 1990 ***(7)***. The first studies of biodoped sol-gel materials reported alkaline phosphatase encapsulated in base-catalyzed silica, and the resulting sol-gel material was opaque with low enzymatic activity. In subsequent work, a sol-gel synthesis route that was able to produce optically transparent monoliths was developed ***(8)***. The proteins copper-zinc superoxide dismutase, cytochrome-*c* (cyt-*c*), and myoglobin were immobilized in the pores of transparent silica glasses, and the biological function and activity of these proteins were monitored spectroscopically. Since that time, a variety of biomolecules, including antibodies, enzymes, other proteins, and even bacteria, have been successfully immobilized in sol-gel matrices, many of which were optically transparent. Research results have been described and summarized in a number of published reviews ***(9–12)***.

One of the most important aspects of using the sol-gel method to encapsulate biomolecules is that the method can be tailored so as not to denature the proteins. That is, the sol-gel-encapsulated biomolecules retain their characteristic reactivities and spectroscopic properties. Some important factors that need to be considered include pH, pore size, and the presence of alcohol. A synthesis protocol that has been successfully used to fabricate optically transparent and biologically active silica gels is illustrated in **Fig. 4**. The protocol consists of (1) mixing alkoxide precursor(s) with water in the presence of dilute acid (catalyst); (2) sonicating the mixture to fully hydrolyze the alkoxide, usually in the absence of alcohol; (3) adding a pH-buffered solution containing the biomolecule of interest; and (4) casting the solution into the desired geometry and shape (monolith or thin film). In this protocol, alcohol concentration is minimized, and the pH of the biomolecule-doped sol is raised to a level that ensures the viability of the biomolecule.

Using the synthesis protocol described in **Fig. 4**, gelation occurs typically between 2 and 30 min. The gelation time depends on a variety of factors, including ionic strength of the buffer, concentration of biomolecules, addition of alcohol (or lack thereof), and temperature. To lengthen the gelation time, one can reduce the buffer ionic strength, reduce the biomolecular concentration, add alcohol, and/or lower the temperature. Another means to lengthening the gelation time is to include an additive such as polyethyelene glycol (PEG) or polyvinyl alcohol. We have successfully extended the gelation time for sols synthesized with the TMOS precursor and biological buffers by tens of minutes or even hours by altering the synthesis conditions. After gelation, polycondensation continues, and the gel network grows in mechanical stability and strength. Retaining sol-gel materials in the wet gel state can be easily accomplished by storing the materials in sealed containers so that pore liquid is not

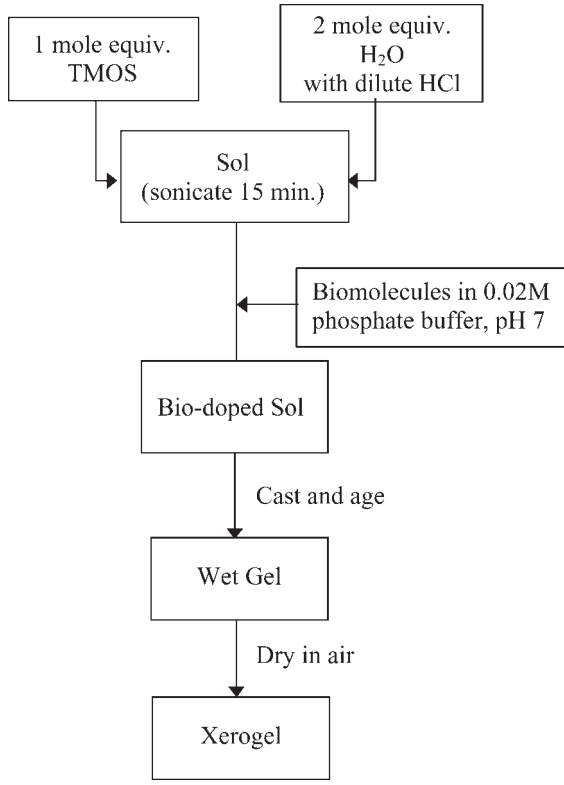

Fig. 4. Synthesis protocol for immobilization of biomolecules in transparent sol-gel silica glasses. TMOS = tetramethylorthosilicate or tetramethoxysilane.

allowed to evaporate. If a xerogel is desired, evaporation should be performed slowly so as to prevent cracking in the matrix.

3. Stabilization of Biomolecules by Sol-Gel Encapsulation

One of the most important benefits of sol-gel immobilization that has emerged is the ability to stabilize biomolecules through encapsulation ***(13–17)***. There is indirect evidence that a biomolecule designs a self-specific pore as the silicate network forms around it during sol-gel hydrolysis and condensation reactions ***(15)***. There is a silicate "cage" that defines the pore according to the size and shape requirements of the biomolecule. Consequently, the biomolecule prevents its surrounding pore from collapsing while the matrix protects the biomolecule from unfolding and aggregation. In addition, the matrix prevents contact with proteases or microorganisms. In the following sections, we review the enhanced stability in terms of thermal, storage, and chemical stability for biomolecules as a result of sol-gel immobilization.

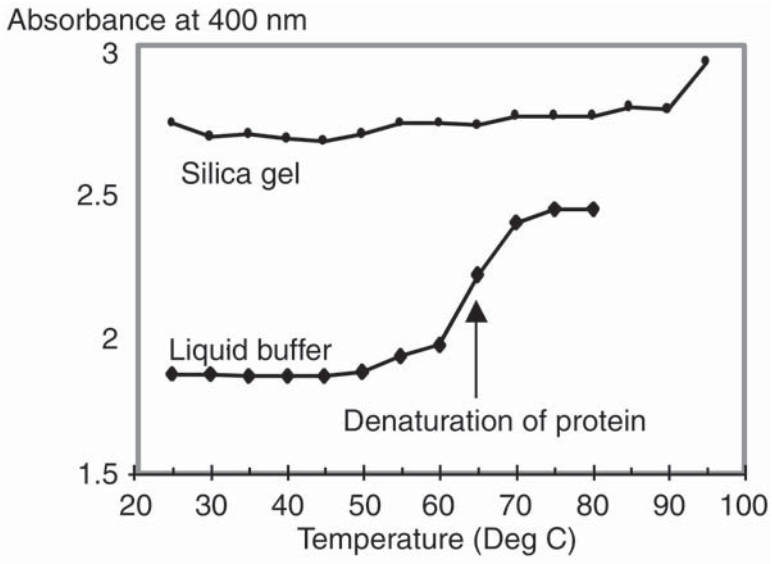

Fig. 5. Thermal denaturation profile of cyt-*c* in liquid buffer and in a wet silica gel shows a substantial improvement in thermal stability as a result of sol-gel encapsulation. The transition temperature, T_m, is approx 65°C in liquid buffer but at least 90°C in the wet gel. (Reproduced from **Ref. *15*** with permission.)

3.1. Thermal Stability

A marked improvement in thermal stability as a result of sol-gel encapsulation has been observed for three flavoprotein oxidases: glucose oxidase, lactate oxidase (LOX), and glycolate oxidase (GLyOX) ***(13)***. When encapsulated in xerogels, where smaller pore sizes were likely to enhance electrostatic interactions between the silicate and the protein, glucose oxidase was reported to be stabilized by immobilization. The extent of the stabilization was impressive; the half-life at 63°C was increased 200-fold on sol-gel encapsulation compared to enzyme in water. Interestingly, LOX and GLyOX were initially destabilized by sol-gel encapsulation. The three oxidases have different p*I* values: 3.8 for glucose oxidase, 4.6 for LOX, and 9.6 for GLyOX. It was apparent that electrostatic interactions between the enzyme and charged silicate matrix caused the destabilization since both LOX and GLyOX experienced a dramatic improvement in stability *if* the enzymes were electrostatically complexed with a base *prior* to sol-gel immobilization. Once electrostatically complexed, LOX experienced a 150-fold increase and GLyOX a 100-fold increase in enzyme half-life at 63°C compared to enzyme in water ***(13)***. These findings show the benefit of increased stability as a result of encapsulation, yet they also under-

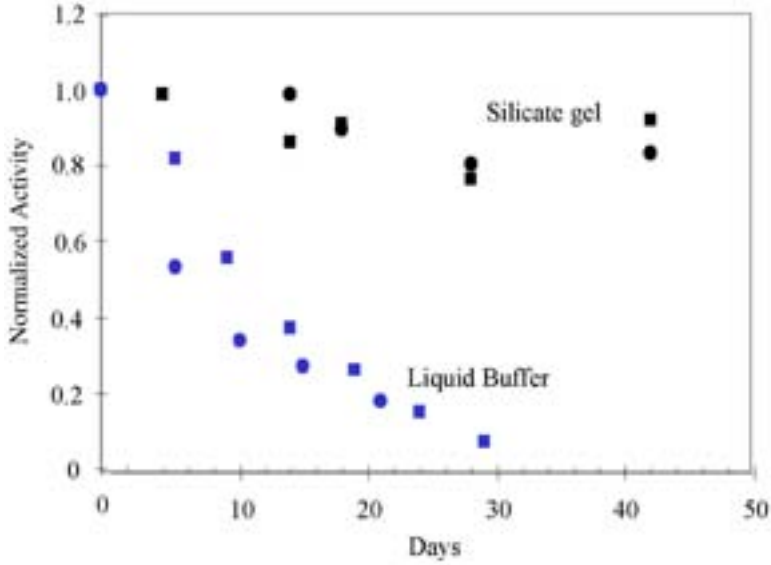

Fig. 6. Normalized enzyme activity of butyrylcholinesterase as a function of storage time at 4°C shows that activity was substantially better retained in the sol-gel-immobilized enzyme than in the free enzyme (enzyme in buffer solution).

score the importance of electrostatic interactions between biomolecules with the highly charged surfaces of the sol-gel-derived matrix.

Increased thermal stability has also been observed in the heme protein cyt-*c* ***(15)***. Thermally induced unfolding of proteins in solution, in general, exhibits a sharp transition over a small temperature range, and the transition point at which half of the molecules are denatured is termed T_m. For cyt-*c*, the unfolding can be monitored using optical absorption of the heme Soret band. As shown in **Fig. 5**, T_m for cyt-*c* in liquid buffer was approx 65°C, whereas T_m for cyt-*c* in the sol-gel matrix was at least 90°C**.** It is possible that the sol-gel-encapsulated cyt-*c* was stable beyond 90°C because boiling of the buffer led to gel cracking at approx 95°C.

3.2. Storage Stability

Whereas thermal stability studies were conducted at elevated temperatures, the storage stability of proteins and enzymes was evaluated at or below room temperature. In experiments with cholinesterase, sol-gel-immobilized enzyme retained enzymatic activity during storage significantly better than enzyme in buffer solution. **Figure 6** shows the activity of butyrylcholinesterase as a function of storage time at 4°C. As seen, the sol-gel-encapsulated enzyme lost almost no activity after 40 d of storage, whereas the enzyme in solution experienced a steady decline in activity during the same period.

3.3. Chemical Stability

Improved chemical stability is also possible. Studies have shown that antibodies immobilized via the sol-gel route better retained their ability to bind antigen after exposure to acid compared with antibodies immobilized via traditional surface attachment. After exposure to 0.01 *N* HCl (pH approx 2.0) for 24 h, sol-gel-encapsulated antitrinitrotoluene (anti-TNT) antibodies experienced essentially no loss in their ability to bind TNT, whereas antibodies immobilized via traditional surface attachment experienced >30% loss ***(16)***.

Results of the chemical stability of cyt-*c* in alcohol indicated that this heme protein partially denatured (unfolded) in buffered solutions with <60 vol% methanol (MeOH), with the degree of denaturation increasing as the amount of methanol increased. Furthermore, at concentrations >60 vol% MeOH, aggregation occurred, depending on the buffer. When encapsulated in silicate gels, however, protein denaturation (unfolding) owing to MeOH was fully reversible; the protein reverted to its native form when samples were soaked in pure buffer. Moreover, protein aggregation did *not* occur for the sol-gel-immobilized protein even when the gels were soaked in pure methanol for several weeks ***(18)***. The results confirm that isolating biomolecules in the pores of the matrix prevented aggregation and at least partially constrained the mobility of the protein.

3.4. Other Considerations

The collective results have shown that, at least for some proteins and enzymes, sol-gel encapsulation has led to a marked improvement in stability. The exact mechanism is not yet understood, although isolation of biomolecules in the pores of the matrix prevents protein aggregation, a known denaturation pathway ***(19)***. Moreover, the matrix may protect the protein from unfolding. It has also been demonstrated that additives present in sol-gel matrices may help stabilize encapsulated biomolecules. For example, PEG added to sol-gel matrices enhanced the activity in lipase ***(20)*** and the half-life of trypsin, and acid phosphatase ***(21)***. There are, however, important considerations if the sol-gel route is selected. The first is the electrostatic interactions between the biomolecule, especially its "active site," and the silicate matrix, because both are likely to be highly charged. Another consideration is that the observed rates of reactions are likely to be lower owing to diffusion limitations. Finally, depending on the size of the immobilized biomolecule, the effect of protein crowding may result in destabilization of the protein conformation ***(22)***.

4. Case Study of Stabilization Owing to Sol-Gel Encapsulation: Enzyme Creatine Kinase

We present here a case study of the stabilization of an enzyme as a direct result of sol-gel encapsulation. The enzyme creatine kinase (CK) is a key

enzyme in cellular energetics. It exists as a dimer held together by hydrogen bonds, with a total mol wt of 82 kDa. The enzyme catalyzes the following reaction:

$$\text{creatine phosphate} + \text{ADP} \overset{\text{CK}}{\rightleftharpoons} \text{creatine} + \text{ATP} \quad (1)$$

To monitor the enzyme activity (rate of reaction), it is extremely difficult to measure the generation of adenosine triphosphate (ATP) directly. As an alternative, the generation of ATP can be measured by coupled enzyme reactions using the enzymes hexokinase and glucose-6-phosphate dehydrogenase (G-6-P dehydrogenase), as described in the following reactions:

$$\text{ATP} + \text{glucose} \overset{\text{hexokinase}}{\rightleftharpoons} \text{Glucose-6-phosphate} + \text{ADP} \quad (2)$$

$$\text{Glucose-6-phosphate} + \text{NADP}^+ \overset{\text{G-6-P dehydrogenase}}{\rightleftharpoons} \text{Gluconate-6-phosphate} + \text{NADPH} \quad (3)$$

When these three reactions are coupled, the rate of formation of NADPH is proportional to the rate of formation of ATP in a linear fashion. The concentration of NADPH can be measured by its absorbance at 340 nm. In the experimental testing of the enzymatic activity of CK, the CK enzyme was the only component immobilized in the sol-gel silica matrix. The solid CK-doped gel was then immersed in a liquid buffer containing the required substrates creatine phosphate, glucose, adenosine 5'-diphosphate (ADP), and $NADP^+$; the required enzymes hexokinase and glucose-6-phosphate dehydrogenase; and a thiol activator, *N*-acetylcysteine. The results showed that the CK enzyme was stabilized owing to encapsulation in sol-gel silica and that there were unusual temperature effects on its activity ***(17)***. These features are discussed in the following sections.

4.1. Long-Term Storage at Room Temperature

Silica gel monoliths with immobilized CK were prepared and stored in near-neutral pH buffer solution at room temperature for as long as 6 mo. As a comparison, CK in liquid buffer was also stored under the same conditions. **Figure 7** shows the relative activity of the enzyme in the sol-gel matrix compared with in liquid buffer. The activity in both the sol-gel monoliths and in solution was normalized to the initial rate. As seen in **Fig. 7**, the encapsulated enzyme retained 90% of its activity after about 5 mo. Thereafter, the activity began to decline and decreased to 50% of its maximum value after 6 mo. By contrast, the activity of CK in liquid buffer dropped to approx 50% of its original activity after only 10 d of storage at room temperature.

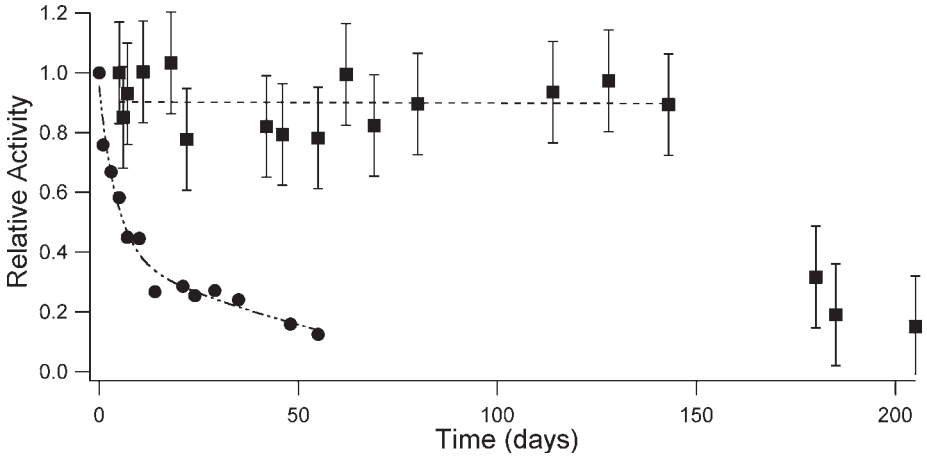

Fig. 7. Relative activity as a function of time for CK when stored at room temperature in pH 7.0 HEPES buffer solution (●) and in sol-gel silica (■) shows that the enzyme had enhanced storage stability as a result of sol-gel encapsulation. The maximum activities per milligram of enzyme for the solution and sol-gel were 0.2 and 7×10^{-5}, respectively. (Reproduced from **Ref. *17*** with permission.)

4.2. Effect of Elevated Temperature and Increase in Activity Following Heating

CK in sol-gel monoliths and buffer solutions were stored at 37, 47, and 60°C for varying lengths of time to evaluate enzyme stability. At the elevated temperatures, for both monoliths and solution, there was a faster loss in CK activity as the temperature was increased. There was, however, significantly higher activity for the sol-gel-encapsulated CK compared with CK in solution at all temperatures. For example, at 60°C, no activity was observed in the CK solution after 1 h, whereas the sol-gel-immobilized enzyme still retained 50% activity after 5 h of heating. Similarly, at 47°C, activity in the solution dropped to essentially zero after about 1 d, whereas the sol-gel-immobilized enzyme retained 50% of its activity after 5 d of heating. Furthermore, the activity remained at approx 50% of its maximum value after 12 d. **Figure 8** shows a comparison of CK activity in both sol-gel monolith and buffered solution after heating at 47°C.

One unusual and unexpected observation from our results was that CK sol-gel monoliths that were heated exhibited a sharp initial *increase* in activity, which was then followed by a gradual decrease. This phenomenon was observed at all elevated temperatures (i.e., 37, 47, and 60°C). The increase in

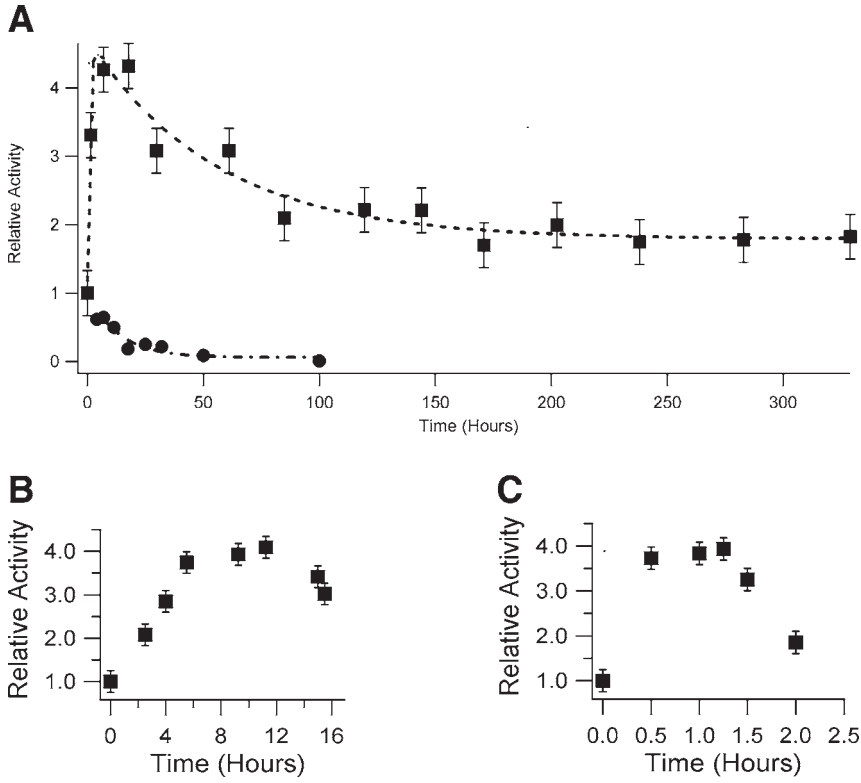

Fig. 8. **(A)** Relative activity as a function of time for CK heated at 47°C in solution (●) and in sol-gel silica (■) shows that the activity in solution decreases immediately, but the activity in sol-gel silica increases before it decreases. **(B)** Activity vs time as a function of heat treatment at 47°C in a CK-doped wet silica gel. **(C)** Activity vs time as a function of heat treatment at 60°C in a CK-doped wet silica gel. (Reproduced from **Ref.** ***17*** with permission.)

activity as a result of heat treatment is shown in **Fig. 8**. The apparent activation energy for the activity enhancement was 2.6 ± 0.6 kJ/mol. The activity increased generally about fourfold as a result of heat treatment. Note that heating the enzyme in liquid buffer did not cause an increase in the activity but, rather, caused an immediate decrease.

The average pore sizes of the sol-gel monoliths were determined using nitrogen adsorption and desorption isotherms. The pore size, pore volume, and surface area as a function of temperature are listed in **Table 1**. There was a relatively narrow pore size distribution in which 80% of the pore volume was within ±10% of the average pore size. The nitrogen adsorption and desorption

Table 1
Pore Size as Function of Heating for Sol-Gel Monoliths

Heating condition	Average pore size (nm)	Pore volume (m^2/g)	Surface area (m^2/g)
Room temperature	8.3	2.0	900
37°C for 3 h	8.8	1.9	780
47°C for 3 h	9.3	2.2	800
60°C for 3 h	10.9	2.2	730

data indicate that there were heat-induced changes in the silica matrix. The pore size increased as a function of temperature, which offers a materials-based explanation for the increase in enzyme activity in the heat-treated samples. With a larger pore size, the enzyme was able to rearrange to a more desirable conformation. In the synthesis of the sol-gel monoliths, gelation occurred on the order of minutes. Although the material experienced a liquid-to-solid transition at gelation, polycondensation continued to occur. As the matrix forms around the enzyme, the enzyme molecules may not be trapped in their native state. By enlarging the pores, the process of enzyme rearrangement becomes more favorable. Maintaining an elevated temperature for an extended period of time, however, induces enzyme denaturation, resulting in a decrease in activity. There are, therefore, two opposing effects, which may explain why the initial activity increased with short-term heating whereas the activity decreased with long-term heating.

To monitor the structural changes and maintenance of the structural integrity of CK, circular dichroism (CD) spectra were taken. CD utilizes circularly polarized light to probe the secondary structure (α helixes and β sheets) of proteins. CD spectra are sensitive to conformational changes and are a common spectroscopic method for studying protein structure ***(23)***. The CD spectra of CK in buffer solution and sol-gel monoliths (with and without heat treatment) were obtained, as shown in **Fig. 9** ***(17)***. The CD spectrum of the enzyme in liquid buffer, which represents the properties of unconfined enzyme in its native state, exhibited a minimum at 220 nm. The CD spectrum of sol-gel-encapsulated enzyme (no heat treatment) showed a minimum at 225 nm, indicating that a large fraction of the enzyme was in a different, nonnative conformational state. On heating the monoliths for 3 h at 37, 47, or 60°C, however, the CD minimum of 220 nm was restored. We can infer from these results that, with heating, the encapsulated enzyme was able to revert to a more native conformation (i.e., the secondary structure of the enzyme became more like that of the enzyme in solution). Enabling the enzyme structure to match more

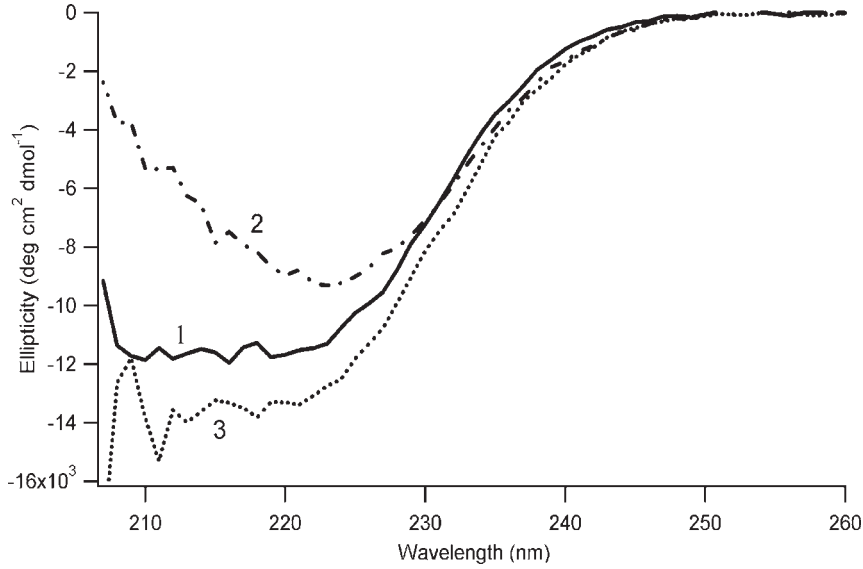

Fig. 9. CD spectra of CK in (1) a freshly made solution, (2) an unheated sol-gel silica monolith, and (3) a monolith heated for 3 h at 47°C. The spectra suggest that the enzyme is confined in a nonnative conformation on initial encapsulation, but after heating the monolith for 3 h, the enzyme conformation becomes more like that of free enzyme (enzyme in solution). (Reproduced from **Ref. *17*** with permission.)

closely its native state may explain why there was an initial increase in its activity.

In a second set of experiments, we monitored the thermal transitions of CK by monitoring changes in the ellipticity at 220 nm (characteristic wavelength) as a function of temperature. Ellipticity is an indication of the α-helical content, and protein unfolding is indicated by an increase in ellipticity. As seen in **Fig. 10** ***(17)***, on heating the monolith and solution to 90°C, the encapsulated enzyme did not fully denature like the enzyme in solution. The midpoint temperature of the unfolding transition, termed T_m, was 75°C for the CK in solution, whereas T_m could not be determined for the monoliths because the enzyme did not unfold completely. In other words, the sol-gel-immobilized CK did not unfold to the same extent as CK in solution. When the temperature was cooled to 20°C, there was virtually no change in ellipticity, indicating that in both cases protein unfolding was not reversible. Nevertheless, these results clearly show that when immobilized in the pores of the sol-gel matrix, the enzyme was able to better withstand thermal denaturation.

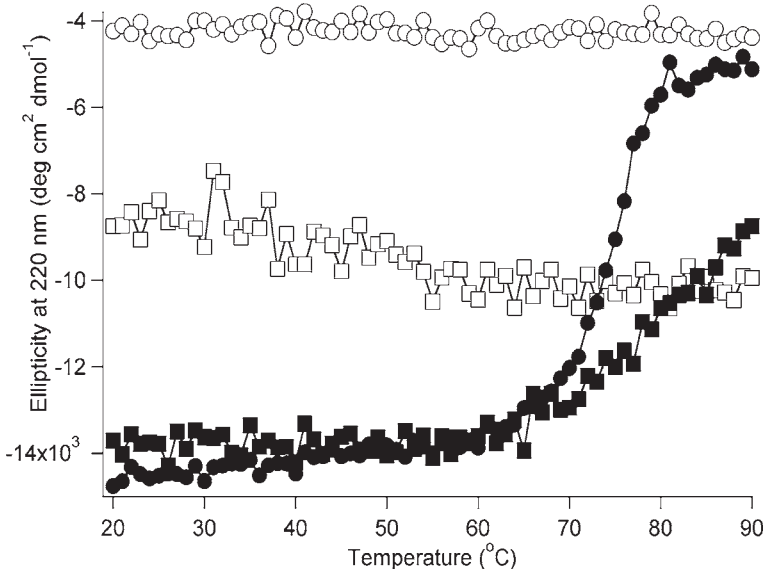

Fig. 10. Thermal unfolding transition of CK in monoliths and in solution monitored by ellipticity at 220 nm: (●) solution during heating; (○) solution during cooling; (■) sol-gel monolith during heating; (□) sol-gel monolith during cooling. The sol-gel-encapsulated enzyme unfolded to a lesser extent compared with free enzyme (enzyme in solution), but in both cases the denaturation was irreversible. The sample was heated at 2°C/min from 20 to 90°C and then cooled from 90 to 20°C. (Reproduced from **Ref. *17*** with permission.)

4.3. Matrix–Enzyme Surface Interactions

The body of work with CK suggests that the enzyme may act as a pore template during the sol-gel process; that is, the matrix forms around the enzyme during gelation. As to the mechanism of stabilizing CK using sol-gel immobilization, it is plausible to assume that there are favorable interactions between the enzyme and the silica matrix. The outer surface of CK contains more positively charged patches than negative patches, as shown by electron density calculations *(24)*. When sol-gel silica is immersed in buffer of near-neutral pH, the silica walls are negatively charged, because the p*I* of silica is approx 2 ***(4)***. Therefore, electrostatic attraction between the silica matrix surface and the enzyme surface is expected. Although the outer surface of CK interacts significantly with the matrix, the active site of the enzyme does not. The active site of CK is embedded in the interior of the enzyme and experiences essentially no interaction with the silica. It is important that the active site not be altered or blocked in order to retain maximum enzyme activity. The combination of exte-

rior structural stabilization caused by enzyme–pore wall electrostatic interactions and the absence of significant perturbations of the active site in a cleft that is spatially separated from the surface results in a stabilized and active biomaterial ***(17)***.

5. Photochemical Coenzyme Regeneration in Sol-Gel Matrices

For many enzymes, a cofactor (also referred to as a coenzyme) is required, and this is true of dehydrogenase enzymes, which require NAD or NADP as a cofactor (**Eq. 4**):

$$\text{Reduced substrate} + \text{NAD(P)}^+ \overset{\text{dehydrogenase}}{\rightleftharpoons} \text{Oxidized substrate} + \text{NADP(H)} + \text{H}^+ \quad (4)$$

In optical sensing, enzyme activity in dehydrogenase enzymes can be measured conveniently because the reduced form of the coenzyme, NADH or NADPH, fluoresces. Sensors based on this reaction, however, cannot operate continuously without a renewable supply of the coenzyme. We have shown in recent work that a photooxidizer can be incorporated into the sol-gel matrix, along with the enzyme and cofactor, to regenerate by oxidation the reduced cofactor ***(25)***. The organic dye thionine was selected as the photooxidizing agent, because it is stable in the silica matrix, retains its excited-state properties, and is compatible and unreactive with the other components.

Thionine, thio$^+$, absorbs light in the visible range with λ_{max} = 596 nm (**Eq. 5**). In solution, excited thionine, *thio$^+$, oxidizes NADH (**Eq. 6**). As NADH is oxidized, the fluorescence emission of the excited thionine is quenched. Therefore, by exciting thionine (thio$^+$) using visible light (596 nm), it is possible to regenerate NAD$^+$.

$$\text{thio}^+ + h\nu_{596\text{nm}} \xrightarrow{k_a} {}^*\text{thio}^+ \quad (5)$$

$${}^*\text{thio}^+ + \text{NADH} \xrightarrow{k_q} \text{thio} + \text{NAD}^+ \quad (6)$$

The enzyme isocitrate dehydrogenase (ICDH) was used as a model dehydrogenase in this research because the Gibbs free energy of the ICDH reaction strongly favors the oxidation of isocitrate, thereby reducing experimental complications from back reactions ***(26)***. ICDH catalyzes the oxidation of isocitrate to α-ketoglutarate using NADP$^+$ as the electron acceptor (**Eq. 7**):

$$\text{isocitrate} + \text{NADP}^+ \xrightarrow{\text{ICDH}} \alpha\text{-ketoglutarate} + \text{CO}_2 + \text{NADPH} + \text{H}^+ \quad (7)$$

The scheme for photochemical oxidation of NADPH by thionine coupled to the enzymatic reaction of ICDH is shown in **Fig. 11**.

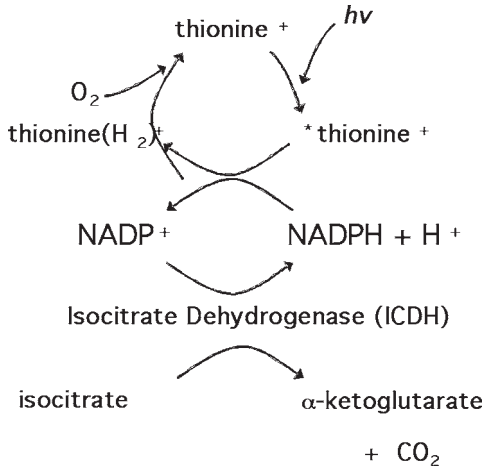

Fig. 11. Enzyme cofactor regeneration for continuous isocitrate oxidation. The photochemical oxidation of NADPH by thionine is coupled to enzymatic oxidation of isocitrate by ICDH. When thionine is excited, it reacts with NADPH to reform $NADP^+$. The regenerated $NADP^+$ becomes available for another isocitrate oxidation. (Reproduced from **Ref. *25*** with permission.)

We first established that NADPH undergoes a reaction similar to NADH with thionine (**Eq. 6**) in that the fluorescence of thionine is quenched as it oxidizes NADPH. The fluorescence emission spectra of thionine in buffer solution and encapsulated in wet silica gels showed essentially no difference, indicating that the optical properties of the thionine photooxidizer itself were not altered as a result of encapsulation. When NADPH-doped silica gels and NADPH buffer solutions were exposed to excited thionine, fluorescence quenching was observed in both the gels and solution. **Figure 12** shows the NADPH concentration, expressed as a percentage of the initial NADPH concentration, over time in the presence of excited thionine (*thio$^+$). The oxidation of NADPH can be described by a decay constant, $k_{oxidize}$, and the rate of oxidation of NADPH was about one order of magnitude slower in the sol-gel matrix. $k_{oxidize}$ was $8.8(\pm1.0) \times 10^{-4}$ s^{-1} in sol-gel silica, compared with $9.8(\pm2.9) \times 10^{-3}$ s^{-1} for buffer solution. The slower observed rate in the sol-gel material may be explained by mass transport limitations. NADPH was immobilized in the gel, whereas thionine was added at time 0 and needed time to diffuse through the pores of the network.

The photochemical oxidation of NADPH can be coupled to the enzymatic oxidation of isocitrate by ICDH (**Fig. 11**). ICDH and thionine were coencapsulated in wet silica gels and incubated with $NADP^+$, and isocitrate was then

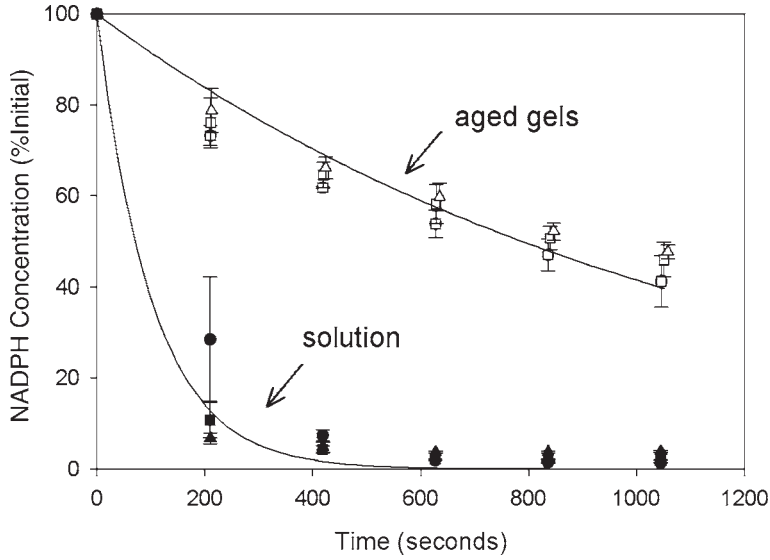

Fig. 12. Disappearance of NADPH during exposure to excited thionine in buffer solution and in wet silica gels. The NADPH concentration is expressed as a percentage of the initial NADPH concentration at time 0. Open symbols show the decrease in NADPH in wet gels, and closed symbols show the decrease in NADPH in solution. Three starting NADPH concentrations were used for each sample type: (○) wet gel, 120 μ*M* NADPH; (□) wet gel, 80 μ*M* NADPH; (△) wet gel, 40 μ*M*; (●) buffer solution, 120 μ*M* NADPH; (■) buffer solution, 80 μ*M* NADPH; (▲) buffer solution, 40 μ*M* NADPH. The data for the six conditions were fit individually to a single exponential decay, $y = 100e^{-bt}$. The decay parameter, *b*, for the wet gels and the solution samples was $8.8(\pm 1.0) \times 10^{-4}$ s^{-1} and $9.8(\pm 2.9) \times 10^{-3}$ s^{-1}, respectively. (Reproduced from **Ref. *25*** with permission.)

injected into the sample at different times. As shown in **Fig. 13**, at each injection of enzyme substrate, the ICDH reaction was observed by the production of NADPH, as indicated by an increase in its fluorescence. When thionine was excited, NADPH was oxidized, resulting in a decrease in its fluorescence. Moreover, the enzymatic reduction of $NADP^+$ to NADPH by ICDH followed by the photochemical oxidation of NADPH to $NADP^+$ by thionine can be cycled. We generated a calibration curve to correlate the NADPH produced as a function of isocitrate concentration and the curve was essentially linear (**Fig. 14**). The data presented in **Figs. 13** and **14** show that a photo-oxidizer can indeed regenerate the NADPH coenzyme, and that photochemical regeneration is possible in a bioactive solid-state silica glass ***(25)***. The collective results suggest that it is possible to utilize dehydrogenase enzymes as optical biosensors

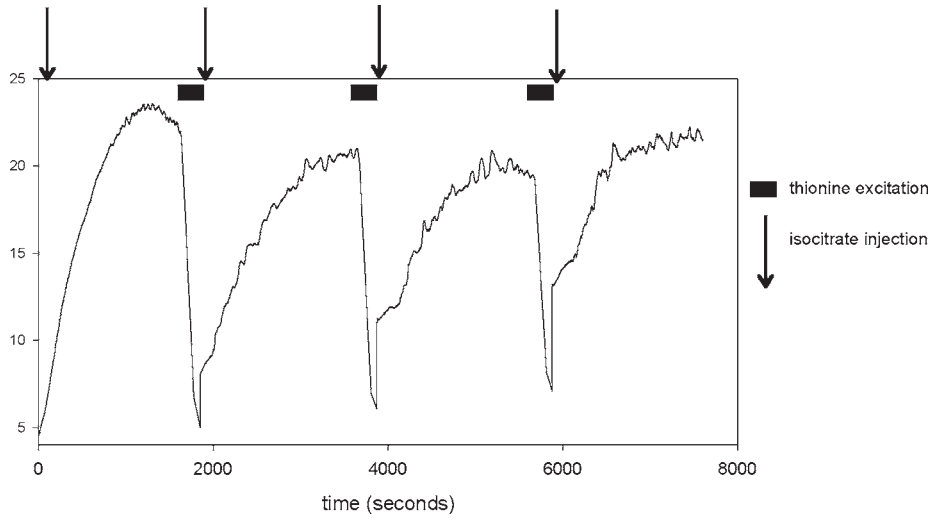

Fig. 13. Repeated ICDH reactions in a sol-gel silica monolith. ICDH, thionine, and $NADP^+$ were encapsulated in a silica gel, and isocitrate was injected onto the gel at the times indicated by the arrows. To monitor the enzyme oxidation of isocitrate, the fluorescence at 460 nm was measured, which indicates generation of NADPH. Subsequently, thionine was excited (at the times indicated by the solid bars) to induce the oxidation of NADPH back to $NADP^+$. This process could be repeated for at least four cycles. (Reproduced from **Ref. *25*** with permission.)

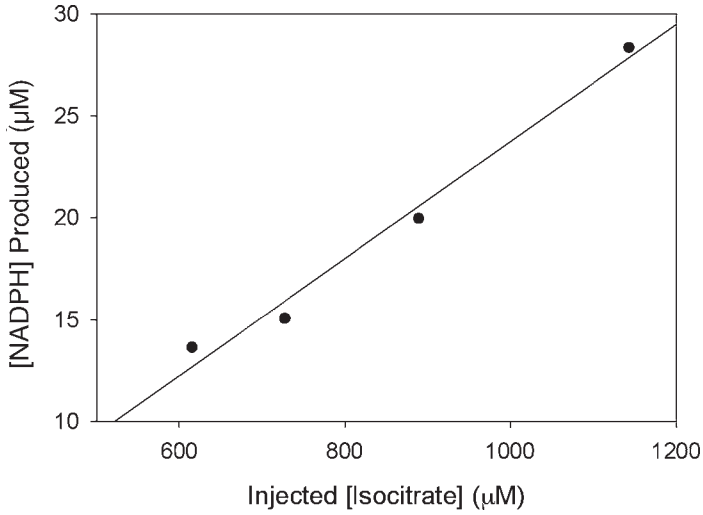

Fig. 14. Calibration curve generated from repeated measurements using the same ICDH-doped gel. The maximum NADPH concentration produced during each cycle is plotted as a function of isocitrate concentration, and a linear curve was observed. (Reproduced from **Ref. *25*** with permission.)

without compromising the continuity of sensor function owing to depletion of coenzyme.

6. Biosensing Elements Using Biologically Active Sol-Gel Thin Films

The potential use of sol-gel-based materials as sensing elements has made these materials the subject of intensive study ***(27,28)***. Although it is possible to use monoliths, for biosensing applications, the use of thin films is preferred. The primary reason is that thin films have a reduced diffusion length for the target analyte, and, therefore, there is a greatly reduced response time, because diffusion distance varies with $t^{1/2}$. The sol-gel matrix has an interconnected network of pores and presents a tortuous path for diffusion of analytes. For thin films, there is an important interplay among porosity and pore size, diffusion coefficient, and response time ***(29)***.

Sol-gel thin films are usually deposited on substrates using either dip coating or spin coating. In dip coating, the thickness can be generally controlled by the withdrawal speed, and it is possible to fabricate coatings with excellent optical transparency. Moreover, it is possible to dip coat onto substrates with a variety of geometries, from planar substrates to optical fibers. If spin coating is used, the thickness can be tailored using the spin rate, and, again, films can have excellent optical transparency.

The fabrication of high-quality sol-gel thin films with functional and active biomolecules is by no means trivial. Generally, biomolecules prefer a near-neutral pH and low-alcohol environment. Under these conditions, the condensation reaction in sol-gel synthesis is accelerated, leading to rapid gelation. A major factor in thin film synthesis is that a reasonable gelation time is required, especially for dip coating. One of the most effective means not only to lengthen the gelation time, but also to lower the viscosity of the sol, is the addition of alcohol. Large and delicate proteins can be particularly sensitive to the presence of alcohol, but apparently some proteins, such as antibodies, still retain their biological function. The fabrication of reproducible thin films with uniform thickness is also necessary if these materials are to be used on a large scale. One advantage of sol-gel coatings is that by matching the coating material with the substrate (e.g., silica coatings on silica substrates), strong adhesion between coating and substrate can be attained.

We have successfully prepared biologically active thin films with immobilized antibodies. The encapsulation of antibodies in sol-gel matrices has been studied extensively ***(16,30–40)*** although only limited work has been performed with thin films. The synthesis protocol for thin films is similar to that for monoliths, except for the addition of methanol to the silica sol and buffered protein mixture. The thin films were deposited on glass substrates by dip coat-

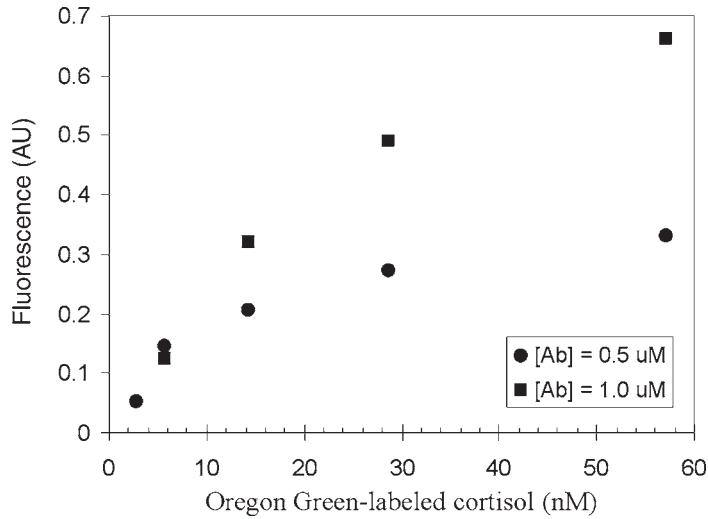

Fig. 15. Fluorescence signal as a function of Oregon Green–cortisol concentration for sol-gel silica thin films containing 0.5 or 1.0 μ*M* anticortisol antibody. The sol-gel-encapsulated antibodies retained their ability to bind antigen, and by increasing the antibody concentration, higher signals can be obtained. (Reproduced from **Ref. *41*** with permission.)

ing. We encapsulated anticortisol antibodies in sol-gel silica thin films and used these materials as sensing elements in an immunoassay for cortisol ***(41)***. The antibody-doped thin films were of excellent quality and optical transparency, with a thickness of approx 1 μm for films in the "wet" state, and a thickness of approx 0.5 μm for films in the "dried" state. Although a significant amount of methanol was used (approx 30 vol%) in the dip-coating solution, the immobilized antibodies retained the ability to bind their target antigen (cortisol in this case). In our experiments, antibody-antigen binding was detected optically using fluorescent Oregon Green–labeled cortisol. Oregon Green is a derivative of fluorescein and experiences excitation and emission in the visible region (495 and 527 nm, respectively). As seen in **Fig. 15**, with a constant antibody concentration in the thin films, the fluorescence signal increased with increasing concentration of labeled antigen. Moreover, by raising the antibody concentration in the thin films, one can obtain higher optical signals.

Note that all experiments were conducted with "wet" films, in which pore sizes remain relatively large. When films were allowed to dry fully, no antibody-antigen binding could be observed. We conducted competitive immunoassays for cortisol using the anticortisol-doped silica thin films. In these immunoassays, in which labeled and unlabeled antigen compete for a fixed number of antibody molecules, the measured signal varies logarithmically with

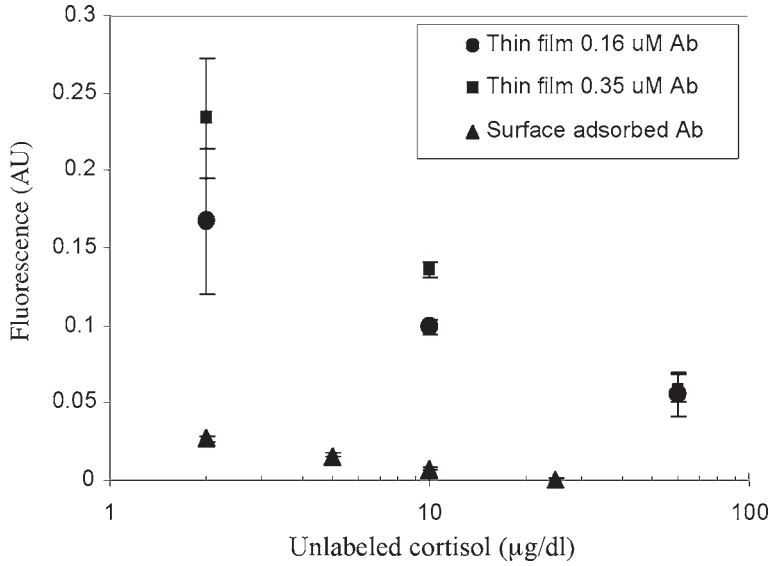

Fig. 16. Calibration curves from competitive immunoassays conducted with sol-gel silica thin films containing anticortisol and with surface-adsorbed anticortisol. With sol-gel encapsulation, we were able to obtain substantially higher signals because of the ability to immobilize a substantially higher number of biomolecules per unit area compared to traditional monolayer surface adsorption. (Reproduced from **Ref.** ***41*** with permission.)

unlabeled antigen concentration, and the slope is negative ***(42,43)***. The competitive immunoassays with anticortisol sol-gel thin films exhibited the expected behavior; a calibration curve with a negative slope was obtained (**Fig. 16**). Moreover, with a higher antibody concentration in the thin film, higher signals were achieved.

When immobilizing biomolecules, one distinct advantage of sol-gel encapsulation is the ability to create 3D architectures. With traditional immobilization methods, such as surface adsorption or covalent attachment, monolayer coverage of the biomolecule is usually obtained. With sol-gel encapsulation, however, one can achieve a substantially higher number of biomolecules per unit area because of the 3D nature of the bioactive material. The total number of biomolecules immobilized depends on the thickness of the material. This feature was demonstrated by comparing competitive immunoassay results for anticortisol encapsulated in sol-gel thin films (approx 1 μm thickness) and surface adsorbed on polystyrene. As seen in **Fig. 16**, the fluorescence signals from the sol-gel films were as much as 10 times higher than those measured using surface-adsorbed antibody.

Finally, there is a distinct advantage with thin films in terms of reduced response times. The immunoassay with anticortisol thin films (approx 1 μm thickness) required an incubation of only 20 min, and experiments showed that a plateau in the signal was reached after approx 10 min (data not shown). When analogous immunoassays were performed with anticortisol-doped silica monoliths of 1-mm thickness, the required incubation time for the assay was at least 3 h. For biological assays, therefore, thin films are far more effective than monoliths because limitations owing to analyte diffusion through the porous matrix can be minimized.

7. Conclusion

Immobilization of biomolecules in sol-gel-derived matrices leads to a wide variety of bioactive materials. The flexible processing inherent in sol-gel synthesis and the ability to use chemical modifications are attributes that make sol-gel methods an attractive platform for biosensors. The prospect of using sol-gel immobilization to better retain the activity of enzymes and enhance the chemical and thermal stability of proteins makes these bioactive materials especially promising. Some important considerations for the widespread use of these materials in biosensing include the size limitations on target analytes, continuous biosensing, and incorporation into devices. With current synthesis procedures, relatively large biomolecules (e.g., proteins) are immobilized in the pores of the matrix, but small analytes diffuse through the porous network. For future applications, a nanostructured material that permits the diffusion of some large biomolecules and yet allows other large biomolecules to remain encapsulated in the pores would be highly desirable. The feasibility of using sol-gel-based biosensors for continuous sensing has not been adequately explored, because most research has been directed at demonstrating proof of concept. Future work directed at continuous monitoring, along with incorporating sol-gel-sensing elements into actual devices, will enable these materials to make a wide impact on biosensing technology.

Acknowledgments

We greatly appreciate the contributions of Dr. Dorothy Nguyen, Dr. Jenna Rickus, Jing C. Zhou, James R. Lim, Maria H. Chuang, and Pauline Chang to the work described in this review. We also gratefully acknowledge support for this research from NSF (DMR 0103952 and DMR 0099862) and NASA (NAG9-1252). This work was also partially supported by the Center for Cell Mimetic Space Exploration, a NASA University Research, Engineering and Technology Institute, through award no. NCC 2-1364.

References

1. Hench, L. L. and West, J. K. (1990) The sol-gel process. *Chem. Rev.* **90,** 33–72.
2. Brinker, C. J., Keefer, K. D., Schaeffer, D. W., and Ashley, C. S. (1982) Sol-gel transition in simple silicates. *J. Non-Cryst. Solids* **48,** 47–64.
3. Brinker, C. J. and Scherer, G. W. (1985) Sol-gel glass: gelation and gel structure. *J. Non-Cryst. Solids* **70,** 301–322.
4. Brinker, C. J. and Scherer, G. W. (1990) *The Physics and Chemistry of Sol-Gel Processing*, Academic, San Diego.
5. Sakka, S. (1982) Gel method for making glass, in *Treatise on Materials Science and Technology*, vol. 22, (Herman, H. and Tomozawa, M., eds.), Academic, New York, pp. 129–167.
6. Rickus, J. L., Dunn, B., and Zink, J. I. (2002) Optically based sol-gel biosensor materials, in *Optical Biosensors: Present and Future* (Ligler, F. S. and Rowe-Taitt, C. A., eds.), Elsevier Science, Amsterdam, The Netherlands, pp. 427–456.
7. Braun, S., Rappoport, S., Zusman, R., Avnir, D., and Ottolenghi, M. (1990) Biochemically active sol-gel glasses—the trapping of enzymes. *Mater. Lett.* **10,** 1–5.
8. Ellerby, L. M., Nishida, C. R., Nishida, F., Yamanaka, S. A., Dunn, B., Selverstone Valentine, J., and Zink, J. I. (1992) Encapsulation of proteins in transparent porous silicate-glasses prepared by the sol-gel method. *Science* **255,** 1113–1115.
9. Avnir, D., Braun, S., Lev, O., and Ottolenghi, M. (1994) Enzymes and other proteins entrapped in sol-gel materials [review]. *Chem. Mater.* **6,** 1605–1614.
10. Livage, J., Coradin, T., and Roux, C. (2001) Encapsulation of biomolecules in silica gels [review]. *J. Phys. Condensed Matter* **13,** R673–R691.
11. Gill, I. (2001) Bio-doped nanocomposite polymers: sol-gel bioencapsulates [review]. *Chem. Mater.* **13,** 3404–3421.
12. Zink, J. I., Valentine, J. S., and Dunn, B. (1994) Biomolecular materials based on sol-gel encapsulated proteins. *N. J. Chem.* **18,** 1109–1115.
13. Chen, Q., Kenausis, G. L., and Heller, A. (1998) Stability of oxidases immobilized in silica gels. *J. Am. Chem. Soc.* **120,** 4582–4585.
14. Heller, J. and Heller, A. (1998) Loss of activity or gain in stability of oxidases upon their immobilization in hydrated silica: significance of the electrostatic interactions of surface arginine residues at the entrances of the reaction channels. *J. Am. Chem. Soc.* **120,** 4586–4590.
15. Lan, E. H., Dave, B. C., Fukuto, J. M., Dunn, B., Zink, J. I., and Valentine, J. S. (1999) Synthesis of sol-gel encapsulated heme proteins with chemical sensing properties. *J. Mater. Chem.* **9,** 45–53.
16. Lan, E. H., Dunn, B., and Zink, J. I. (2000) Sol-gel encapsulated anti-trinitrotoluene antibodies in immunoassays for TNT. *Chem. Mater.* **12,** 1874–1878.
17. Nguyen, D. T., Smit, M., Dunn, B., and Zink, J. I. (2002) Stabilization of creatine kinase encapsulated in silicate sol-gel materials and unusual temperature effects on its activity. *Chem. Mater.* **14,** 4300–4306.
18. Miller, J. M., Dunn, B., Valentine, J. S., and Zink, J. I. (1996) Synthesis conditions for encapsulating cytochrome C and catalase in SiO2 sol-gel materials. *J. Non-Cryst. Solids* **202,** 279–289.

19 Eggers, D. K. and Valentine, J. S. (2001) Molecular confinement influences protein structure and enhances thermal protein stability. *Protein Sci.* **10,** 250–261.
20 Kawakami, K. and Yoshida, S. (1995) Sol-gel entrapment of lipase using a mixture of tetramethoxysilane and methyltrimethoxysilane as the alkoxide precursor—esterification activity in organic media. *Biotechnol. Techniques* **9,** 701–704.
21 Shtelzer, S., Rappoport, S., Avnir, D., Ottolenghi, M., and Braun, S. (1992) Properties of trypsin and of acid-phosphatase immobilized in sol-gel glass matrices. *Biotechnol. Appl. Biochem.* **15,** 227–235.
22 Eggers, D. K. and Valentine, J. S. (2001) Crowding and hydration effects on protein conformation: a study with sol-gel encapsulated proteins. *J. Mol. Biol.* **314,** 911–922.
23. Schmid, F. X. (1990) *Protein Structure: A Practical Approach*, IRL Press, Oxford, UK.
24 Nayal, M., Hitz, B. C., and Honig, B. (1999) GRASS: a server for the graphical representation and analysis of structures. *Protein Sci.* **8,** 676–679.
25. Rickus, J. L., Chang, P. L., Tobin, A. J., Zink, J. I., and Dunn, B. (2004) Photochemical coenzyme regeneration in an enzymatically active optical material. *J. Phys. Chem. B.* **108,** 9325–9332.
26 Lehninger, A. L., Nelson, D. L., and Cox, M. M. (1993) *Principles of Biochemistry*, Worth Publishers, New York.
27 Maccraith, B. D., McDonagh, C., McEvoy, A. K., Butler, T., Okeeffe, G., and Murphy, V. (1997) Optical chemical sensors based on sol-gel materials—recent advances and critical issues. *J. Sol-Gel Sci. Technol.* **8,** 1053–1061.
28. Maccraith, B. D., McDonagh, C. M., Okeeffe, G., McEvoy, A. K., Butler, T., and Sheridan, F. R. (1995) Sol-gel coatings for optical chemical sensors and biosensors. *Sens. Actuators B Chem.* **29,** 51–57.
29 McDonagh, C., Bowe, P., Mongey, K., and MacCraith, B. D. (2002) Characterisation of porosity and sensor response times of sol-gel-derived thin films for oxygen sensor applications. *J. Non-Cryst. Solids* **306,** 138–148.
30. Altstein, M., Aharonson, N., Segev, G., Ben-Aziz, O., Avnir, D., Turniansky, A., and Bronshtein, A. (2000) Sol-gel-based enzymatic assays and immunoassays for residue analysis. *Italian J. Food Sci.* **12,** 191–206.
31. Bronshtein, A., Aharonson, N., Avnir, D., Turniansky, A., and Altstein, M. (1997) Sol-gel matrixes doped with atrazine antibodies—atrazine binding properties. *Chem. Mater.* **9,** 2632–2639.
32. Doody, M. A., Baker, G. A., Pandey, S., and Bright, F. V. (2000) Affinity and mobility of polyclonal anti-dansyl antibodies sequestered within sol-gel-derived biogels. *Chem. Mater.* **12,** 1142–1147.
33 Grant, S. A. and Glass, R. S. (1999) Sol-gel-based biosensor for use in stroke treatment. *IEEE Trans. Biomed. Eng.* **46,** 1207–1211.
34 Jiang, D. C., Tang, J., Liu, B. H., Yang, P. Y., and Kong, J. L. (2003) Ultrathin alumina sol-gel-derived films: allowing direct detection of the liver fibrosis markers by capacitance measurement. *Anal. Chem.* **75,** 4578–4584.
35. Jordan, J. D., Dunbar, R. A., and Bright, F. V. (1996) Aerosol-generated sol-gel-derived thin films as biosensing platforms. *Anal. Chim. Acta* **332,** 83–91.

36 Roux, C., Livage, J., Farhati, K., and Monjour, L. (1997) Antibody-antigen reactions in porous sol-gel matrices. *J. Sol-Gel Sci. Technol.* **8,** 663–666.
37. Shabat, D., Grynszpan, F., Saphier, S., Turniansky, A., Avnir, D., and Keinan, E. (1997) An efficient sol-gel reactor for antibody-catalyzed transformations. *Chem. Mater.* **9,** 2258–2260.
38 Turniansky, A., Avnir, D., Bronshtein, A., Aharonson, N., and Altstein, M. (1996) Sol-Gel entrapment of monoclonal anti-atrazine antibodies. *J. Sol-Gel Sci. Technol.* **7,** 135–143.
39 Vazquez-Lira, J. C., Camacho-Frias, E., Pena-Alvarez, A., and Vera-Avila, L. E. (2003) Preparation and characterization of a sol-gel immunosorbent doped with 2,4-D antibodies. *Chem. Mater.* **15,** 154–161.
40. Wang, R., Narang, U., Prasad, P. N., and Bright, F. V. (1993) Affinity of antifluorescein antibodies encapsulated within a transparent sol-gel glass. *Anal. Chem.* **65,** 2671–2675.
41. Zhou, J. C., Chuang, M. H., Lan, E. H., Dunn, B., Smith, S. M., and Gillman, P. L. (2004) Immunoassays for cortisol using antibody-doped sol-gel silica. *J. Mater. Chem.* **14,** 2311–2316.
42. Ashkar, F. S. (1983) *Radiobioassay*, CRC Press, Boca Raton, FL.
43. Pesce, A. J. and Kaplan, L. A. (1987) *Methods in Clinical Chemistry*, C. V. Mosby, St. Louis, MO.